From Microscopic Interactions to Macroscopic Laws of Cluster Evolution

Markos A. Katsoulakis[1,*] and Dionisios G. Vlachos[2,]

[1]*Department of Mathematics and Statistics, University of Massachusetts, Amherst, Massachusetts 01003-3110*
[2]*Department of Chemical Engineering, University of Massachusetts, Amherst, Massachusetts 01003-3110*

(Received 8 July 1999)

We derive macroscopic governing laws of growth velocity, surface tension, mobility, critical nucleus size, and morphological evolution of clusters, from microscopic scale master equations for a prototype surface reaction system with long range adsorbate-adsorbate interactions.

PACS numbers: 66.30.–h, 61.46.+w, 82.20.Wt

Intermolecular forces often determine macroscopic phenomena in a wide spectrum of applications ranging from catalysis, to epitaxial growth of materials, to agglomeration of particles. In particular, attractive interactions result in formation of clusters which subsequently affect macroscopic dynamics. For example, cluster and more generally pattern formation of adsorbates and their evolution on catalytic surfaces result in deviations of rate expressions from classical mass action kinetic laws, and affect dynamics and reactor design. These examples underscore the need for understanding the role of microscopic interactions in macroscopic dynamics. In this Letter, we focus on cluster evolution in catalytic processes.

Surface reactions on single crystals of catalysts have traditionally been modeled using continuum-type diffusion-reaction models, where the adlayer has been assumed to be spatially uniform. This mean-field approach treats interactions only phenomenologically. Molecular simulations, such as lattice-gas Monte Carlo (MC), are best suited to model intermolecular forces along with their influence on catalytic kinetics [1].

A major disadvantage of MC simulations is their computational intensity which limits calculations to small length scales and short times. In contrast, many experimental techniques used to probe layers of adsorbates are limited to micrometers, and real systems are of even larger macroscopic length scales. Recent developments on the complex relations of microscopic Ising-type systems and their approximating, meso- and macroscopic theories, in a general nonequilibrium statistical mechanics context, include [2–6]. Furthermore, a mesoscopic model for catalytic surfaces was developed in [7].

Here we present a general and systematic mathematical approach to derive macroscopic scale laws starting from microscopic scale information through the mesoscopic *local mean-field theory*. Such an approach can provide information over relatively large length scales which are experimentally more easily accessible. The mathematical techniques developed so far regarding the derivation of macroscopic scale laws [2,4–6] mostly address Ising systems equipped with a single updating mechanism, although some simple combined mechanisms were also studied (see references listed in [4–6]). The novelty of the results reported in this Letter lies with addressing more realistic systems where *multiple* microscopic mechanisms such as surface diffusion, reaction, and adsorption or desorption coexist and interact. Our mathematical techniques describe concretely this combined effect on the macroscopic scale laws through derived Kubo-Green formulas for the cluster mobility and surface tension. The prototype physical model we consider consists of the molecular adsorption of species A onto a catalytic surface. The adsorbed species A^* can desorb back into the fluid phase, diffuse on the surface, or react through a unimolecular surface reaction to give product B. Nonideality in the adsorbed layer is caused by adsorbate-adsorbate attractive interactions which, when strong enough, can lead to a multivalued isotherm [1,8].

We will first present a straightforward generalization of the mesoscopic theory developed in [7], when all microscopic processes occur simultaneously. For long range interatomic potentials, Arrhenius desorption dynamics, and Metropolis surface diffusion, the mesoscopic local mean-field equation for the coverage u is

$$u_t - D\nabla \cdot [\nabla u - \beta u(1-u)\nabla J_m * u] - [k_a p(1-u) - k_d u \exp(-\beta J_d * u)] + k_r u = 0. \quad (1)$$

Here J_d and J_m are the intermolecular potentials for surface desorption and migration. Furthermore, D is the diffusion constant, k_r, k_d, and k_a denote, respectively, the reaction, desorption, and adsorption constants, p is the partial pressure of the gaseous species A, and $J * u$ denotes the convolution. In this Letter we focus on studying the asymptotics, and the resulting cluster evolution, of two special cases of (1), when $k_r = 0$: first, the Fickian diffusion case,

$$u_t - D\Delta u - [k_a p(1-u) - k_d u \exp(-\beta J_d * u)] = 0, \quad (2)$$

and second, the case presented in [7], where $J_d = J_m = J$. Although the prototype system we consider is two dimensional, we carry out all our calculations in $\mathbf{R}^n$.

Next we state some of the basic properties of (1) and (2). Steady state solutions of either equation satisfy the algebraic equation $f(x) := \alpha(1-x) - xe^{-\lambda x} = 0$, where

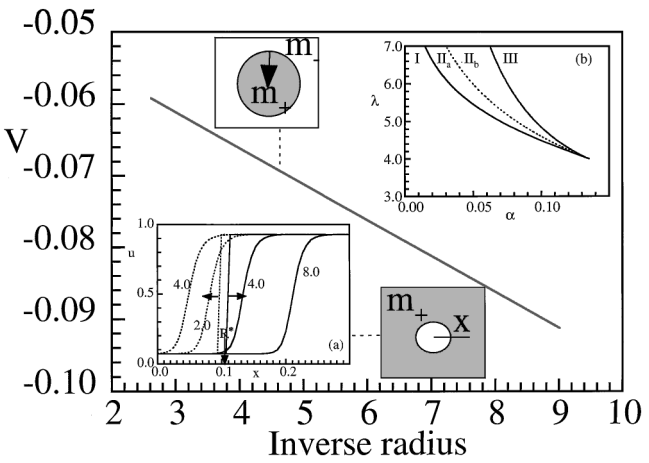

FIG. 1. Velocity of a shrinking cluster of the dense phase (gray circle) vs its inverse radius. Inset (a) shows snapshots of two clusters of dilute phase (white circle) of different initial radii at times t/ϵ indicated. The parameters are $\lambda = 6$ and $\alpha = 0.0497$. Inset (b) shows the phase diagram for the adsorption-desorption model, in the absence of a surface reaction.

$\alpha = k_a p/k_d$ and $\lambda = J_0\beta, J_0 = \int J(r)\,dr$. Figure 1(b) (cf. [7]) shows schematically the phase diagram as a function of the dimensionless pressure α and the interaction parameter λ. Outside the cuspy envelope, in region I (respectively, III) adsorbates form a dilute (respectively, dense) phase. Within the cuspy envelope (region II), both phases can exist and $f(x)$ has three roots $m_- < m_0 < m_+$, where m_+ and m_- correspond to the dense and the dilute phases of the system, respectively. The dynamics of cluster evolution depends on the subregion separated by the *stationary coexistence* curve [the dotted line in Fig. 1(b)], satisfying $\alpha = e^{-\lambda/2}$.

One-dimensional standing and traveling waves for Eqs. (1) and (2) are crucial in our analysis below, since they connect high and low density phases across a cluster boundary. These special solutions are of the type $u(r,t) = q(r \cdot e - ct), r \in \mathbf{R}^n$, where e is any unit vector, $q = q(\xi), \xi \in \mathbf{R}$, and $c = c(\alpha,\lambda)$ denotes the speed of the wave. There are no general rigorous results available on the existence of traveling waves for (1); however, some numerical simulations for identical interaction potentials $J_m = J_d = J$ were carried out in [7]. In this special case, on the line of stationary coexistence, the standing wave q of (1) satisfies

$$-\tilde{J} * q + \frac{1}{\beta}\ln\left(\frac{q}{1-q}\right) = -\frac{1}{2}J_0, \qquad q(\pm\infty) = m_\pm . \tag{3}$$

In addition, $\dot{q} > 0$, where $(\cdot)$ denotes the derivative with respect to the ξ variable. From here on we assume that the interaction potential J is non-negative and radially symmetric, and we define $\tilde{J}(\zeta) = \int_{\mathbf{R}^{n-1}} J[(\zeta^2 + |r'|^2]^{1/2}\,dr'$, $\zeta \in \mathbf{R}$. The existence of such standing waves is shown in [3].

It turns out (using the methods in [9]) that (2) admits monotone traveling wave solutions $q = q(\xi)$ with speed $c = c(\alpha,\lambda)$, satisfying

$$-c(\alpha,\lambda)\dot{q} - D\ddot{q} - k_a p(1-q) + k_d q \exp[-\beta\tilde{J} * q] = 0, \qquad q(\pm\infty) = m_\pm . \tag{4}$$

We now focus on the main results of this Letter, regarding the evolution of clusters in the long space-time asymptotics of (1) and (2). We consider two distinct scaling regimes of the equations: (i) When the parameters (α,λ) lie away from the stationary coexistence line [see Fig. 1(b)], the speed of propagation of clusters is nonzero as the traveling wave analysis indicates. We scale space-time in (2) as $(r,t) \mapsto (r\epsilon^{-1}, t\epsilon^{-1})$; thus the transitions between high and low density regions (described by traveling waves) become sharper for $\epsilon \ll 1$, and clear cluster boundaries emerge, denoted by Γ_t where t is the rescaled time. (ii) When the parameters (α,λ) lie within $O(\epsilon)$ of the line of stationary coexistence, then the wave $q = q^\epsilon$ moves slowly, i.e., $c = c^\epsilon(\alpha,\lambda) = O(\epsilon)$ and so do the corresponding clusters. To capture effectively this slow motion, along with possible effects due to the cluster geometry we scale space-time in (2) as $(r,t) \mapsto (r\epsilon^{-1}, t\epsilon^{-2})$. Physically these scalings represent a long characteristic time compared to the desorption time, i.e., taken as $\epsilon^{-1}k_d^{-1}$ and $\epsilon^{-2}k_d^{-1}$, respectively, and a ratio of diffusion length to macroscopic length proportional to ϵ times the square root of a constant, still denoted by D in the scaled equations.

Initially we concentrate on the study of Eq. (2). We will carry out the analysis first for the case when the parameters (α,λ) lie within $O(\epsilon)$ of the line of stationary coexistence. We consider the solution ansatz for (2) in the scaling regime (ii),

$$u(r,t) = q^\epsilon\big(\epsilon^{-1}d(r,t)\big) + \epsilon Q\big(\epsilon^{-1}d(r,t)\big) + O(\epsilon^2), \tag{5}$$

where q^ϵ is the traveling wave, solving (4) with speed $c = c^\epsilon(\alpha,\lambda)$. Q denotes a higher order corrector, which is identified by solving an appropriate "cell" problem [see (6) below]. It is the condition guaranteeing the solvability of the cell problem that yields the Kubo-Green formulas for the surface tension and mobility below. We now define the signed distance function $d = d(r,t)$ from a point $r \in \mathbf{R}^n$ to the cluster boundary Γ_t; see [5] for precise definitions. We remind the reader that the normal velocity V of Γ_t is given by $V = d_t$, while the outward normal unit vector of Γ_t is $-\Delta d$ and its mean curvature is $\kappa = -\Delta d$. It is possible to show with formal asymptotics (and also rigorously) that the local equilibrium ansatz (5) describes a solution of (2) around a cluster boundary [see also the

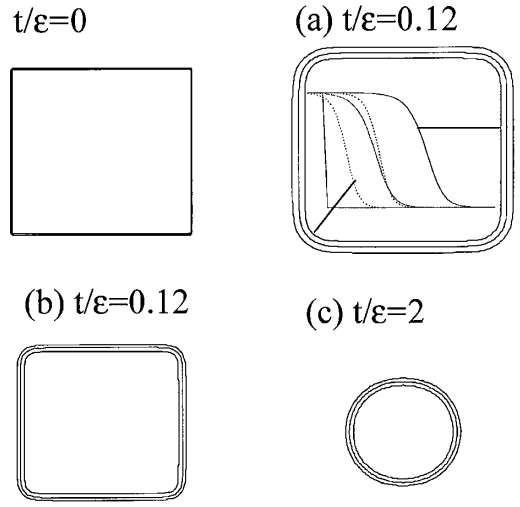

FIG. 2. Contours at values 0.25, 0.50, and 0.75 of u for an initially square cluster of the dense phase embedded in the dilute phase, when $\lambda = 6$ and (a) $\alpha = 0.07$ (subregion II_b), (b) $\alpha = 0.037$ (subregion II_a), and (c) $\alpha = 0.05$ (near the coexistence line), at indicated times. The initial cluster covers 25% of the total simulation area.

inset of Fig. 2(a) for a numerical validation of the ansatz, even past singularities of the cluster boundary]. It remains to identify the morphological evolution of the clusters.

Inserting the ansatz (5) into the rescaled (2) and ignoring the higher order terms, we obtain

$$\mathcal{L}_D Q = [k_d q \exp(-\beta \tilde{J} * q)]^{-1} \dot{q} \left\{ d_t - D\Delta d - \frac{c^\epsilon(\alpha,\lambda)}{\epsilon} \right\} - \frac{\beta}{2} \int J(r') \dot{q}(\cdot + r' \cdot e)(\hat{e} \cdot r')^2 \, dr' \, \Delta d \,, \quad (6)$$

where e and $\hat{e}$ are any two orthogonal unit vectors and q denotes the standing wave for (4) obtained when we set $\epsilon = 0$ in q^ϵ. The operator $\mathcal{L}_D$ is the linearization of (4) around q. The Fredholm theory implies that Eq. (6) is solvable for Q if and only if the right-hand side is orthogonal in $L^2(\mathbf{R})$ to the kernel of the adjoint $\mathcal{L}_D^*$ of $\mathcal{L}_D$. In earlier work [5], where surface diffusion terms were not included, i.e., $D = 0$, the operator $\mathcal{L}_D = \mathcal{L}_0$ is self-adjoint and one easily gets that $\ker \mathcal{L}_0^* = \ker \mathcal{L}_0 = \dot{q}(\cdot)\mathbf{R}$. This is not the case here so we need to study separately $\ker \mathcal{L}_D^*$. Using the implicit function theorem, we can show that there is a solution χ_D of $\mathcal{L}_D^* \chi_D = 0$ when D is small enough. The comparison principle for (2) also implies that in this case $\ker \mathcal{L}_D^* = \chi_D(\cdot)\mathbf{R}$, and $\chi_D > 0$. This result can be extended to any positive diffusion coefficients D by a continuation argument. We now multiply (6) by χ_D and integrate. The left-hand side vanishes since $\ker \mathcal{L}_D^* = \chi_D(\cdot)\mathbf{R}$; thus we have that on the interface $\Gamma_t, d_t = \mu\sigma\Delta d + \mu\Lambda$. This equation readily implies the macroscopic law for the normal velocity V of the cluster boundaries Γ_t,

$$V = -\mu\sigma\kappa + \mu\Lambda \,. \quad (7)$$

The integration against χ_D also yields that the mobility μ and surface tension σ are given by the *Kubo-Green formulas*

$$\mu = \beta \left[\int_{-\infty}^{\infty} \frac{\dot{q}(\xi)\chi_D(\xi)}{D\ddot{q} + k_a p(1-q)} \, d\xi \right]^{-1}, \quad (8)$$

$$\sigma = \frac{D}{\beta} \int_{-\infty}^{\infty} \frac{\dot{q}(\xi)\chi_D(\xi)}{D\ddot{q} + k_a p(1-q)} \, d\xi + \frac{1}{2} \times \int_{-\infty}^{\infty} \int J(r') \dot{q}(\xi + r' \cdot e) \chi_D(\xi) (\hat{e} \cdot r')^2 \, dr' \, d\xi \,. \quad (9)$$

Furthermore, $\Lambda = (h/\beta) \int_{-\infty}^{\infty} \{[1 - q(\xi)]\chi_D(\xi)/D\ddot{q} + k_a p(1-q)\} d\xi$. Note that when $D = 0$, $\chi_D = \dot{q}$. Because of the radial symmetry of J, the right-hand side of (9) is independent of the particular choice of e and $\hat{e}$. Since $\chi_D > 0$ we have that $\mu, \sigma > 0$. The formulas (8) and (9) specify the relationship between the macroscopic properties of the propagating clusters on one hand, and the microscopic parameters on the other.

Similarly one handles cluster evolution away from the line of stationary coexistence. In this case, we substitute the ansatz (5) in (2) under the rescaling (i), where we employ the traveling wave with speed $c = c(\alpha, \lambda)$. Following the previous techniques we have the macroscopic law

$$V = -\epsilon\mu\sigma\kappa + c(\alpha,\lambda) \,. \quad (10)$$

Here the mobility μ and surface tension σ are given by the formulas (8) and (9), when q and χ_D are replaced by their traveling wave counterparts. The derivation of (7) and (10) from (2) is valid even past the formation of front singularities (e.g., sintering of two clusters), since (2) has a comparison principle. For the mathematical techniques necessary, we refer to [5,10]. Similar velocity laws in related scaling regimes were also derived from reaction diffusion equations and Ising spin flip systems [5,11].

We now turn towards the analysis of Eq. (1) in the special case $J_m = J_d = J$, when the parameters (α, λ) lie close to the curve of stationary coexistence. Our techniques apply for all parameter choices with the necessary scaling modifications of (1) outlined earlier in model (2). Proceeding as in the analysis of the Fickian model, we obtain that the normal velocity of the cluster boundaries is given by (7), where the mobility μ and surface tension σ are given by the Kubo-Green formulas

$$\mu = \beta \left[\int_{-\infty}^{\infty} \frac{\dot{q}(\xi)\chi(\xi)}{k_a p(1-q)} \, d\xi \right]^{-1}, \quad (11)$$

$$\sigma = \frac{1}{2} \int_{-\infty}^{\infty} \int J(r') \dot{q}(\xi + r' \cdot e) \chi(\xi) (\hat{e} \cdot r')^2 \, dr' \, d\xi \,, \quad (12)$$

where q is the standing wave (3), and $\Lambda = (h/p\beta) \times (m_+ - m_-)$. Here χ is the solution of $\mathcal{L}^* \chi = 0$, where $\mathcal{L}^*$ denotes the adjoint of the operator obtained from the linearization of (1) around the standing wave q. Since

$\ker \mathcal{M} = \dot{q}(\cdot)\mathbf{R}$, where $\mathcal{M}$ is the linearization of (3) around q, $\mathcal{M}\tau = \tilde{J} * \tau - \frac{1}{\beta}F'(q)\tau$, and $F(q) = \ln[q/(1-q)]$, we readily obtain that χ solves

$$-\left\{q(1-q)\left(\frac{D}{k_a p(1-q)}\chi\right)^{\cdot}\right\}^{\cdot} + \chi = \dot{q}, \qquad \chi(\pm\infty) = 0, \tag{13}$$

and that $\ker \mathcal{L}^* = \chi(\cdot)\mathbf{R}$. Furthermore, by the maximum principle and the fact that $\dot{q} > 0$, we have that $\chi > 0$ and thus $\mu > 0$. Interestingly, comparison of two extreme cases, namely, the equal potentials case and the Fickian case considered above, indicates that macroscopic laws have an explicit dependence on the diffusion constant D only in the Fickian case. This result is typically not considered in the classical nucleation (continuum level) theory.

The Kubo-Green formulas (8), (9), (11), and (12) and the velocity law (7) allow us to calculate explicitly the macroscopic cluster *nucleation radius* R^*, close to the coexistence line. Because of the isotropy of the interaction potentials we obtain that $R^* = \sigma/\Lambda$. Formulas (8), (9), (11), and (12) yield the precise dependence of the critical radius on the microscopics.

To numerically validate the approximation of the mesoscopic equations with the macroscopic interface evolution laws, we have carried out simulations using for illustration the Fickian model (2). On a 151×151 lattice we consider a second-order finite difference discretization scheme of (2) with reflective boundary conditions. Initially, clusters of one phase are embedded in the other phase. The interatomic potential taken from [7] is $(\lambda/\pi r_0^2)\exp(-r^2/r_0^2)$, although other choices are also possible. In the simulations reported here, we take $r_0 = 2/150$ and $\epsilon = 1/600$.

First, simulations were performed for $D = 1$, $\lambda = 6$, and $\alpha = 0.0497$ (in region IIa, near the coexistence line). Figure 1 shows the speed of a shrinking circular cluster (of the dense phase embedded in the dilute phase) versus the inverse of its radius from direct numerical simulations of (2) giving $V = -0.005/R + 0.046$. Within the accuracy of the simulations, the linearity of macroscopic law (7) is confirmed, and the intercept is in excellent agreement with the speed, $\mu\Lambda = 0.0467$, of a 1D traveling wave ($\kappa = 0$), computed independently. Furthermore, using the above estimates, the critical nucleus radius is $R^* = \mu\sigma/\mu\Lambda \approx 0.108$. Two illustrative examples of simulations in Fig. 1(a) confirm this value of R^* when the evolution (growth or shrinking) of dilute phase clusters, embedded in the dense phase, is considered for the same conditions.

As another test of the numerical accuracy of the macroscopic laws, the case of $D = 0$ was considered. By computing the standing wave, the values of μ and Λ were independently computed giving $\mu\Lambda = 0.0216h$. Simulations of 1D traveling waves at various pressures ϵh from the coexistence line gave speeds within 20% of this value. We believe that this agreement can be improved by more accurate computation of $\dot{q}$, by employing, for example, front tracking techniques.

In Fig. 2 we depict contours, i.e., level curves of the solution u of (2) lying between the two steady state solutions $m_\pm$. Note that the asymptotic expansion (5) implies that as $\epsilon \to 0$, all such contours along with the whole transition region between $u \approx m_+$ and $u \approx m_-$ collapse to the sharp cluster boundary Γ_t whose evolution is given by (7) or (10). According to (10), far from the coexistence line, patterns evolve with the traveling wave speed, and curvature effects are only of order ϵ. This is, in fact, seen in Fig. 2 near the corners of a growing cluster in subregion II_b. In contrast, near the coexistence line, curvature effects dominate according to (7).

Further results for other diffusion dynamics (e.g., Arrhenius) and anisotropic interaction potentials can also be obtained. It will also be of interest to compare direct simulations of (7) and (10) using the level-set method [12], to the mesoscopic equations (1) and (2), as well as to the corresponding microscopic Monte Carlo algorithms.

The research of M. A. K. and D. G. V. is partially supported by the National Science Foundation through DMS-9626804, DMS-9801769, and CTS-9702615.

*Corresponding authors.

[1] D. G. Vlachos, L. D. Schmidt, and R. Aris, Surf. Sci. **249**, 248 (1991).
[2] H. Spohn, J. Stat. Phys. **71**, 1081 (1993).
[3] A. De Masi, E. Orlandi, E. Presutti, and L. Triolo, Proc. R. Soc. Edinb. **124A**, 1013 (1994).
[4] A. De Masi, E. Orlandi, E. Presutti, and L. Triolo, Nonlinearity **7**, 633 (1994).
[5] (a) M. A. Katsoulakis and P. E. Souganidis, J. Stat. Phys. **87**, 63 (1997); (b) M. A. Katsoulakis and P. E. Souganidis, Commun. Math. Phys. **169**, 61 (1995).
[6] G. Giacomin and J. L. Lebowitz, SIAM J. Appl. Math. **58**, 1707 (1998).
[7] M. Hildebrand and A. S. Mikhailov, J. Phys. Chem. **100**, 19 089 (1996).
[8] I. Kevrekidis, L. D. Schmidt, and R. Aris, Surf. Sci. **137**, 151 (1984).
[9] X. Chen, Adv. Differential Equations **2**, 125 (1997).
[10] L. C. Evans and J. Spruck, J. Differ. Geom. **33**, 635 (1991).
[11] (a) J. P. Keener and J. J. Tyson, Science **239**, 1284 (1988); (b) L. C. Evans, H. M. Soner, and P. E. Souganidis, Commun. Pure Appl. Math. **35**, 1097 (1992).
[12] S. Osher and J. A. Sethian, J. Comput. Phys. **79**, 12 (1988).